DEM Generation from Multi-View Satellite Images in Sub-Sahel Region

Multi-platform, Multi-scale and Multi-temporal 4D Glacier Monitoring. The Rutor Glacier Case Study

Myrta Maria Macelloni[1], Elisabetta Corte[1(✉)], Andrea Ajmar[3], Alberto Cina[1], Fabio Giulio Tonolo[2], Paolo Felice Maschio[1], and Isabella Nicole Pisoni[1]

[1] DIATI – Department of Environmental, Land and Infrastructure Engineering, Politecnico di Torino, Corso Duca degli Abruzzi 24, 10129 Torino, Italy
{myrta.macelloni,elisabetta.corte}@polito.it
[2] DAD – Department of Architecture and Design, Politecnico di Torino, Viale Pier Andrea Mattioli 39, 10125 Torino, Italy
[3] DIST - Interuniversity Department of Regional and Urban Studies and Planning, Politecnico di Torino, Viale Pier Andrea Mattioli 39, 10125 Torino, Italy

Abstract. At present most alpine glaciers are not in equilibrium with the current climate, as a result they are undergoing a dramatic mass loss. Monitoring glacial variations is crucial to assess the consequences of climate change on the territory. In this work different geomatics techniques are exploited to measure and monitor the Rutor glacier over the years. In this study two different techniques were adopted to generate 3 digital surface models (DSMs): aerial and satellite photogrammetry. Two photogrammetric aerial surveys were carried out: at the end of the hydrological year 2019/20 and at the end of the following hydrological year. Additionally, a very high-resolution satellite stereo pair, acquired by the Pléiades-1A platform in 2017, was processed to assess whether satellite images can be applied to extract the 3D surface of the Rutor glacier. In order to evaluate the Rutor glacier mass-balance throughout the years several reference points were positioned and measured before the 2021 aerial flight. Thanks to the presence of the materialized points the 2021 model is considered as the 'Reference Model' against which subsequent models can be compared for glacier analysis. This model was validated by means of a comparison with the authoritative Regional DSM based on LiDAR surveys. In alpine glaciers, the positioning of artificial square cross target in time invariant areas is crucial to enable a multitemporal 4D analysis. The use of very high-resolution satellite imagery allows large areas to be mapped in 3D, but with lower accuracies proportionally decreasing with respect to slope and exposure.

Keywords: Aerial photogrammetric survey · Satellite · Photogrammetry · 3D · Glacier monitoring · Multi-temporal

E. Borgogno-Mondino and P. Zamperlin (Eds.): ASITA 2022, CCIS 1651, pp. 392–404, 2022.
https://doi.org/10.1007/978-3-031-17439-1_29

1 Introduction

Alpine areas are one of the most affected by climate change. Alpine glaciers recession has remarkable consequences on the water supply of the valley floor sectors, on the production of hydroelectric energy and on the agricultural productivity of the downstream areas [1, 2]. Hence monitoring glacial variations enable the analysis of climate change impact and the assessment of its effects on the territory.

Remote sensing techniques have always been used to investigate glaciers. Satellite images allow the study of glaciers without requiring direct in situ measurements (depending on the positional accuracy requirements), furthermore these can cover extremely wide areas (in the range of hundreds of km^2, including several glaciers) and long archive time-series are potentially available. Nowadays satellite images are widely used in cryosphere studies. Satellite images have been successfully used to study glaciers kinematics and dynamics [3, 4]. However, despite the very high level of detail (with a spatial resolution up to 30 cm) the vertical accuracy may still be limiting for some applications.

Satellite images drawbacks can be overcome with Manned or Unmanned Aerial Vehicles (UAVs) photogrammetry. Aerial photogrammetry allows very high-resolution images (up to few centimeters) to be acquired over areas with limited accessibility. Manned aerial flights are more expensive but, unlike UAVs, they allow to survey much wider areas without requiring a team to be deployed in the field. The acquired very high-resolution imagery can be used to build high resolution 3D point clouds, Digital Surface Models (DSMs) and orthophotos exploiting Structure-from-Motion (SfM) and Multi-View Stereo (MVS) algorithms [5, 6]. These products have been widely employed for applications such as: river flow velocity and discharge estimation [7, 8], mapping hazard related to glacier collapse [9], glacier dynamics [10, 11].

Rutor glacier mass-balance has been monitored since 2004 by ARPA Valle d'Aosta and Fondazione Montagna Sicura. At first, mass-balance measurements were achieved only through direct in situ measurement [12]. Since 2020, with the cooperation of the Glacier Lab of Politecnico di Torino, field work has been integrated with aerial and drone photogrammetry.

To investigate the yearly evolution two photogrammetric manned flights were performed over the Rutor glacier, the first at the end of the hydrological year 2019/20 and the second at the end of the following hydrological year. Moreover, a very high-resolution satellite stereo-pair from the Pléiades constellation was used to assess the feasibility of a satellite-based monitoring. Considering the extent of the monitored areas, UAV photogrammetry is not discussed in this manuscript.

1.1 Case Study

Rutor glacier is Valle D'Aosta's third largest glacier and is one of the most representative due to its geographical position, morphological and glaciological characteristics [12]. It is located at the head of the Dora valley in La Thuile, in north-western Italy, next to the French-Italian border. The Rutor glacier has a surface area of 8,4 km^2 and its longest flow line is 4,68 km long. The glacier descends from its top elevation of 3486 m a.m.s.l. up to the front at 2540 m a.m.s.l. alternating sloping areas with more flat zones. The accumulation zone of Rutor is formed by two large main circuses confined by

rocky ridges and divided by the Vedettes du Rutor. The ablation zone is formed by three tongues, the lowest altitude is reached by the orographic right one.

Rutor glacier has been the object of several studies [13–15] and its mass-balance has been monitored since 2004 by ARPA Valle d'Aosta and Fondazione Montagna Sicura: their analysis confirms that from 2004/05 to 2011/12 the net mass balance has always been negative while for the two hydrological years 2012/13 and 2013/14 mass accumulation exceeded mass loss [12].

2 Materials and Methods

In this study different digital photogrammetry techniques were used. The processed remotely sensed imagery were acquired from a camera carried on a light aircraft and from the Pléiades satellite constellation. The adopted cartographic reference system is ETRF2000 UTM 32 N (EPSG: 6707), while the elevation component refers to the ITALGEO2005 geoid model. When required, datum conversion have been carried out using VERTO IGM transformation approach [16].

2.1 Photogrammetric Flight

Two photogrammetric flights were carried out to survey the Rutor glacier on 30 September 2020 and 13 September 2021. The flights were commissioned to DigiSky, which is a Turin-based EASA certified company. Both flights required about an hour to survey the entire glacier surface, as shown in Fig. 1 [17].

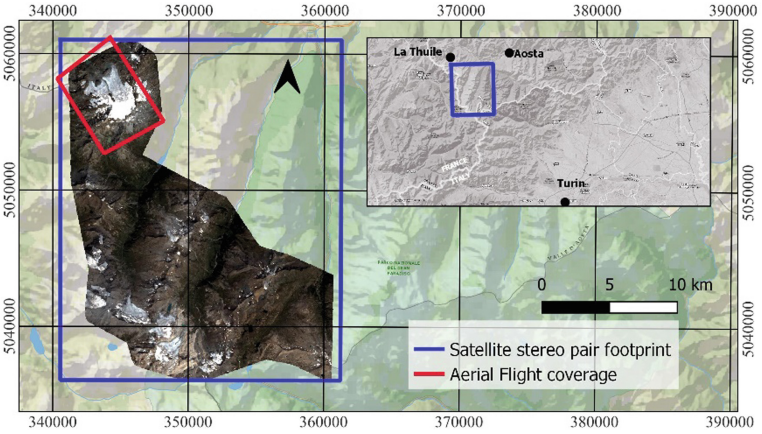

Fig. 1. Satellite (orthophoto and blue rectangle) and aerial 2021 (red rectangle) covered area. Coordinate System: ETRF2000 UTM32N (Color figure online)

The aircraft used to carry out the photogrammetric flights was equipped with a global navigation satellite system (GNSS) antenna, an inertial measurement unit (IMU) with low accuracy and a PhaseOne camera. The PhaseOne camera model is the iXM-RS150F

and was installed under the right wing of the aircraft. This is a medium format camera with a focal length of 50 mm, a sensor size of 40 mm × 53.5 mm and a resolution of 151.3 MP [18].

2.2 Satellite Imagery

ARPA Valle D'Aosta shared with the Glacier Lab of Politecnico di Torino a Pléiades stereo pair acquired on 20/08/2017 at 10:34 UTC characterized by off-nadir angles of ±8° leading to a real GSD of 0,71 m (delivered products are resampled at 0,5 m by the satellite data provider). The sensor installed on the satellite constellation covers the visible and the Near-Infrared (NIR) spectral bands with a spatial resolution of 0,7 m (panchromatic spectral band) and 2,8 m (multispectral spectral bands). The swath field of view is 20 km in nadiral position [19]. The covered surface is 268,468 km^2 in the Aosta Valley region (Fig. 1) close to the borders among Aosta Valley, Piedmont, and France, with different mountainous areas, the Gran Paradiso area and the Rutor glacier.

2.3 Control Points and Measurement Campaigns

Before the second aerial flight, a set of 30 reference points was positioned and measured with artificial square cross targets, measured by means of GNSS surveys. The first survey purpose was to position the targets on the glacier and to determine their position.

Since the purpose of this project is to evaluate the Rutor glacier mass-balance throughout the years and not its displacement, the targets on the glacier were placed on stable areas along the moraines and the rocky ridges, aiming to use these targets as invariant reference points also for future photogrammetric flights. We considered as stable areas the rocky ridges bordering the glacier and the proglacial area, assuming that these are time invariant zones.

To determine the 3D coordinates of the targets, a master station was installed in the barycentric reference point of the glacier and the coordinates of the targets were obtained in Real Time Kinematic (RTK) mode. When internet connectivity is available, HxGN SmartNet GNSS RTK Network was used as Virtual Reference Station (VRS) techniques. Since the points were placed after the first flight, the model of the 30 September 2020 was co-registered to the 2021 model with 18 Ground Control Points (GCPs). The coordinates of these points were extracted from the 2021 model. Among all the 30 measured points, 12 were used as Ground Control Points (GCPs) to orient the photogrammetric flight carried out in 2021 (6 placed on the glacier area and 6 on the proglacial area, Fig. 2a). In addition, the IGM95 (Istituto Geografico Militare) point placed on the Testa del Rutor was used as a GCP for the 2020 and 2021 models.

To build the 3D model from the stereo satellite imagery, 6 GCPs were extracted automatically from the orthophoto obtained from the processing of the aerial survey carried out in 2021 with a Ground Sample Distance (GSD) of 50 cm and a planar accuracy of 9 cm. The height of these GCPs was derived from the 2021 aerial DSM.

To determine the accuracy of the 2020 aerial model with respect to the 2021 one, 10 Independent Check Points (ICP) were used. To check the accuracy of the satellite imagery model, only 2 stereo CPs were selected on the reference 2021 aerial orthoimagery due to the challenging identification of homologues points.

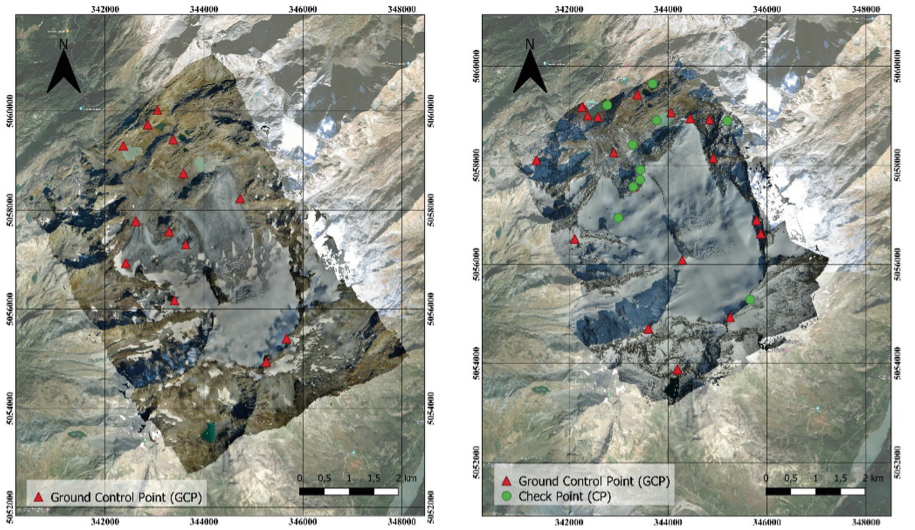

Fig. 2. a) GCP distribution for the 2021 aerial survey; b) GCP and CP distribution for the 2020 aerial survey

2.4 Reference Cartographic Data

In order to determine the accuracy of the DSM obtained from the 2021 aerial survey, a DSM produced in 2008 by Valle d'Aosta was used as reference. This DSM is derived from LIDAR surveys and has a spatial resolution of 2 m. The reference system of the model is ED50/UTM zone 32N (EPSG: 23032). Since the reference system of the 2021 model is ETRF2000, the required Datum conversion was carried out with the Italian ConveRgo software and VERTO approach [16].

2.5 Data Processing

Aerial Photogrammetry. The images acquired during the photogrammetric flights were processed using AgiSoft Metashape Professional v 1.8.1.

After the images were imported and aligned, the markers were manually identified linking the relevant 3D coordinates. The dense point cloud (generated with high resolution settings) is composed by 3.338.453.261 points for the 2021 model and 1.871.761.605 points for the 2020 model. The number of points of the dense cloud of the two models is proportional to the area of the surveys. Once the dense cloud and the mesh were generated, the cartographic products were extracted.

The 2021 model is considered as the 'Reference Model' against which subsequent models can be compared for glacier retreat and melting considerations. To further validate the 2021 model, a comparison with the 2008 LIDAR DSM [18] was carried out.

Satellite Photogrammetry. The Pléiades satellite stereo pair was processed using Geomatica Banff software 2019 edition. The adopted model is the Rational Function Model,

RFM (or RPC, Rational Polynomial Coefficients), a non-parametric math-based model that relates ground 3D coordinates to image 2D coordinates.

After a preliminary pansharpening step (producing a new multispectral dataset at the spatial resolution of the panchromatic band), the satellite stereopair orientation was carried out by automatically identifying reference points from the aerial orthomosaic and the related DSM (to be used both as GCP and CP) and tie points (TPs) (Fig. 3). The automatic identification was manually cross-checked by means of visual interpretation. After the model calculation, the epipolar images are generated and the Digital Surface Model (DSM) and the two orthophotos are extracted. The 3D positional accuracy was estimated on both GCP and CP, as shown in Tables 1 and 2.

Glacier 4D monitoring. Multitemporal DSMs describing the glacier surface allow the glacial mass ablation between two dates to be calculated. In this study four different DSM were used to assess the elevation differences (as well as to evaluate the accuracy of the aerial and satellite surface models in the stable areas).

Lidar (2008) vs Aerial (2021). As mentioned previously, the 2021 aerial model is considered the reference dataset since it was oriented exploiting the artificial targets positioned before the aerial survey. To assess the accuracy and validate the 2021 aerial model, a comparison with the authoritative Regional LIDAR DSM was carried out, as described in Sect. 2.2. The two DSMs are subtracted in a GIS environment to calculate the differences and evaluate the accuracy on the selected time-invariant areas. The difference between the two DSMs on the glacier area provides an estimation of the glacier mass changes.

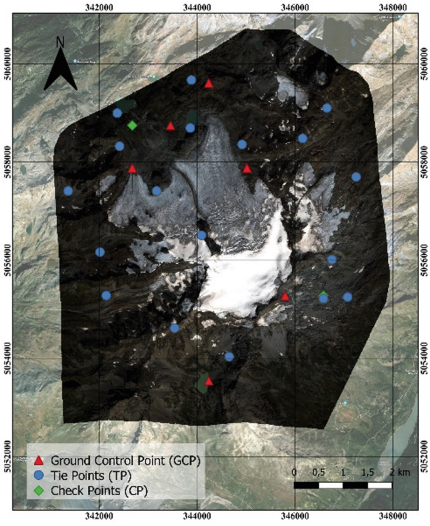

Fig. 3. Satellite GCP and CP model 2020 disposition

Aerial (2020) vs Aerial (2021). The same procedure was applied to subtract the 2021 Aerial DSM from the 2020 Aerial DSM to compare invariant zones and glacier melt in one year. To properly interpret the results, it has to be highlighted that 2020 aerial imagery is characterised by an extensive snow coverage, as clearly visible in the orthophoto.

Satellite (2017) vs Aerial (2021). As far as satellite photogrammetry is concerned, the comparison was carried out between the 2017 Satellite DSM and the 2021 Aerial DSM.

A first qualitative analysis of the elevation differences highlighted that the elevation accuracy seems to be related to the slope. To quantitatively confirm this hypothesis, the elevation differences have been grouped in 5 different slope ranges and the accuracy metrics have been recalculated accordingly (Table 3). Adopting the same approach, the analysis was carried out considering 8 DSM aspect classes (mountainside azimuth) to understand if the illumination condition as well as the relative position of the satellite, with respect to the main orientation of the glacier valley, could impact on the accuracy of the satellite stereo-pair processing (Table 4). The slope and aspect analysis were carried out only on stable areas.

3 Results

3.1 Cartographic Products: Orthophoto and DSM

The following cartographic products were obtained from the Digisky 2021 flight model:

- an Orthophoto with a GSD equal to 0.06 m
- a DSM with a GSD equal to 0.24 m

The following cartographic products were obtained from the Digisky 2020 flight model:

- an Orthophoto with a GSD equal to 0.07 m
- a DSM with a GSD equal to 0.14 m

The following cartographic products were obtained from the Pléiades 2017 satellite photogrammetric model:

- 2 Orthophotos (one for each image of the stereo pair) with a GSD equal to 0.50 m
- a DSM with a GSD equal to 0.50 m.

The residual errors [cm] on GCPs and CPs are shown in Table 1 and Table 2 respectively :

Table 1. Residual errors on GCPs.

Model	N. Points	RMSE X [cm]	RMSE Y [cm]	RMSE Z [cm]
Aerial 2021	13	4,6	2,7	5,5
Aerial 2020	18	24,9	13,7	7,9
Plèiades 2017	6	5,5	15,5	43,5

Table 2. Residual errors on CPs.

Model	N. Points	RMSE X [cm]	RMSE Y [cm]	RMSE Z [cm]
Aerial 2020	10	18,0	18,3	26,2
Plèiades 2017	2	12,4	0,8	0,8

Table 3. Statistics related to slope range (stable areas).

Slope range	Count (pixel)	Mean [m]	Standard deviation [m]
$S < 18°$	4.631.745	−2.89	3.88
$18° < S < 36°$	8.574.643	−2.26	6.00
$36° < S < 54°$	5.625.899	−1.41	7.58
$54° < S < 72°$	2.087.941	0.75	9.86
$S > 72°$	544.735	5.13	12.47

3.2 DSM Comparisons

Lidar (2008) vs Aerial (2021). Considering that the Geoportal DSM is based on airborne LIDAR, as expected, the average difference is about −0.24 m and the standard deviation is 0.42 m on stable areas around the glacier area (Fig. 4A).

Aerial (2020) vs Aerial (2021). The average difference between the DSMs on the stable areas around the lakes area is equal to about 0.09 m and the standard deviation is 0.11 m. The glacier melt estimation highlights the difference of snow ablation between the upper part and the lower part: the east forehead thickness loss is around 4 m/year, 2 m/year on the west forehead and 3–4 m/year on the central forehead (Fig. 4B).

Satellite (2017) vs Aerial (2021). Similarly to studies based on other glaciers, although the morphology of the glaciers is different, the altimetric accuracy seems to decrease with the slope's increase [3]. For selected slope classes on stable areas, the difference between the Satellite and aerial DSM was assessed, and the relevant statistics were calculated (Table 3).

The mean value of difference between the two DSM increases significantly between the slope classes, but more significant is the increase in the standard deviation from 3.8 m to over 12 m for the steepest parts. As a general result, it can be highlighted that the DSM obtained from the satellite images tend to smooth the elevation differences with respect to the reference DSM.

The same approach was adopted to investigate the possible relation between elevation accuracy and terrain aspect, i.e. a thematic map showing the azimuth of the terrain.

There is a clear correlation between the satellite DSM residuals and the terrain aspect, due to possible impact of illumination condition during the stereopair acquisition.

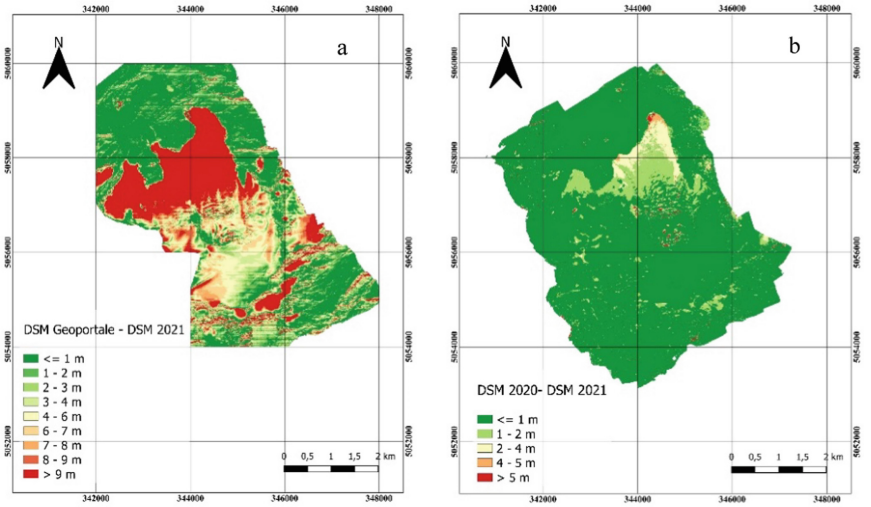

Fig. 4. a) Comparisons between GEOPORTALE VDA and aerial DSM; b) Comparisons between 2020 and 2021 DSM

Moreover, the relation between vertical accuracy and terrain aspect can be also due to the relative satellite/mountainside position, which leads to occluded areas in the stereoscopic pair. It is important to underline that the vast majority of the analysed areas are facing South, making the interpretation of the results less robust.

Table 4. Statistics related to exposure range (stable areas).

Exposure Range	Direction	Count	Mean [m]	Standard Deviation [m]
$-22.5° < E < 22.5°$	North	7.000.022	−5.09	4.76
$22.5° < E < 67.5°$	North-East	969.933	−3.26	5.51

(*continued*)

Table 4. (*continued*)

Exposure Range	Direction	Count	Mean [m]	Standard Deviation [m]
67.5° < E < 112.5°	East	470.927	−1.98	6.22
112.5° < E < 157.5°	South-East	1.027.201	−0.87	6.49
157.5° < E < 202.5°	South	9.087.075	1.1.54	7.70
202.5° < E < 247.5°	South-West	1.352.347	−2.21	5.28
247.5° < E < 292.5°	West	700.060	−3.10	4.92
292.5° < E < 337.5°	North-West	1.436.766	−3.95	4.58

4 Discussion and Conclusion

In this work, photogrammetric approaches based on imagery acquired from aerial and satellite platforms were adopted for a multi-temporal 3D monitoring of the Rutor glacier. For our purposes the positioning and measuring of artificial square cross targets had a crucial role on the analysis. The accuracy of the models depends strongly on the availability of reference points with known 3D accuracy that can be easily pinpointed on the acquired imagery. In glacier environments is really hard to identify points that are stable over time and that can be recognised in different years due to the rapid landscape changes. Moreover, snowfalls can hide the more stable areas surrounding the glacier preventing the identification of the same points in multi-temporal acquisitions. Indeed, this was the case of the 2020 model. Due to the snow coverage on the accumulation area of the Rutor glacier, the search of points along the glacier upper part was a challenging task.

The use of very high-resolution satellite imagery is a theoretically shorter process than processing aerial images and enables much wider areas to be covered, but it presents some disadvantages that have not been fully solved. From the elevation variations perspective, although the measurements are consistent with other analyses, the accuracy is lower with a clear influence of both terrain slope and aspect. Additionally, although rocky areas are considered to be stable over time, these could include areas subject to landslides or partial changes over time. Nevertheless, it is still effective in identifying relevant ($> \pm 5$ m) elevation changes and consequently hot spots were to focus more detailed surveys. In planar terms, the satellite orthoimages allow the retreat of the glacial fronts to be assessed and a comparison with other products to be carried out. In fact, the Rutor front was delineated using the orthophotos obtained from: Digisky and UAV flights models, Pléiades photogrammetric model and the Geoportale VdA [20] (Fig. 5). Further analyses are planned to evaluate the expected improvements when using 30 cm satellite stereopairs.

The relative orientation of the terrain aspect with respect to the satellite azimuth has an impact on the 3D accuracy and therefore is a limitation in the use of satellite imagery in glacier monitoring. The influence of terrain aspect could be overcome by combining targeted drone surveys in areas characterised by lower accuracy or, where possible, by

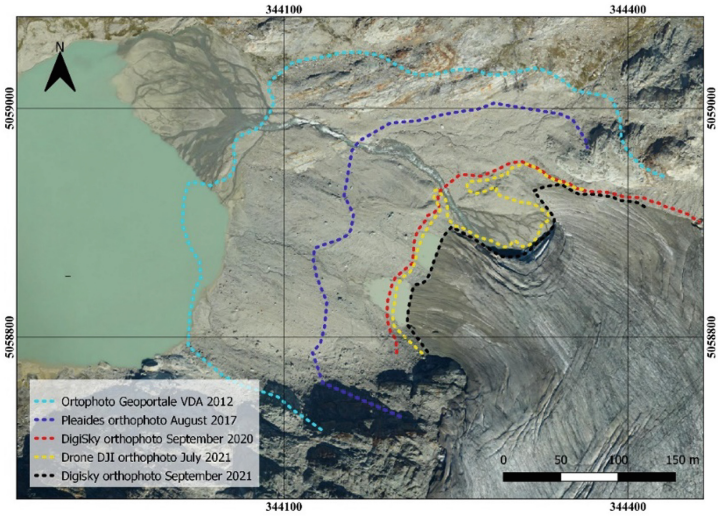

Fig. 5. Multitemporal analysis of east glacial forehead retreat.

choosing the optimal azimuth among the available archive satellite images covering the area under investigation.

The availability of DSM with an elevation accuracy of few centimeters enable to estimate the ablation rate, that for the Rutor case study is as average 4 m/year on the east glacial forehead, 2 m/year on the west forehead and in the range from 3 to 4 m/year on the central forehead. This outcome is consistent with the results of the comparison with the 2008 Geoportal LIDAR DSM that estimates the melting of the east front up to 60 m in 13 years. This is also possible considering the different amount of snow melted per year and the consideration of 2020 as a year of less melting of the Aosta Valley glaciers. (ARPA VDA mass balances preliminary results).

The strong dependence of elevation precision from terrain slope and aspect suggest to carefully evaluate the use of satellite photogrammetry with actual GSD larger than 0.5 m for monitoring glaciers with centimetric accuracy, mainly depending on of glaciers morphology and orientation. Although the validation of the model on stable areas did not lead to the expected results, the gentle slope of the glacier allows us to qualitatively estimate the mass melted as about 20 m in the period 2017–2021 on the front, a figure consistent with those of other comparisons. The work carried out can be further developed, collaborating with ARPA Valle D'Aosta for increasingly accurate and multidisciplinary glacier 4D monitoring. In addition, another group of experts carried out geophysics and hydrological surveys not addressed in this work during the summer campaigns. The integration of these data in the 3D model would enable a complete analysis of the evolution of the glacial environment.

References

1. Beniston, M., et al.: The European mountain cryosphere: a review of its current state, trends, and future challenges. Cryosphere **12**, 759–794 (2018)

2. Gobiet, A., Kotlarski, S., Beniston, M., Heinrich, G., Rajczak, J., Stoffel, M.: 21st century climate change in the European Alps-A review. Sci. Total Environ. **493**, 1138–1151 (2014)
3. Giulio Tonolo, F., Cina, A., Manzino, A., Fronteddu, M.: 3D glacier mapping by means of satellite stereo images: the belvedere glacier case study in the Italian alps. Int. Arch. Photogrammetry Remote Sens. Spat. Inf. Sci. ISPRS Arch. **43**, 1073–1079 (2020)
4. Fieber, K.D., Mills, J.P., Miller, P.E., Clarke, L., Ireland, L., Fox, A.J.: Rigorous 3D change determination in Antarctic Peninsula glaciers from stereo WorldView-2 and archival aerial imagery. Remote Sens. Environ. **205**, 18–31 (2018)
5. Westoby, M.J., Brasington, J., Glasser, N.F., Hambrey, M.J., Reynolds, J.M.: "Structure-from-Motion" photogrammetry: a low-cost, effective tool for geoscience applications. Geomorphology **179**, 300–314 (2012)
6. Seitz, S.M., Curless, B., Diebel, J., Scharstein, D., Szeliski, R.: A comparison and evaluation of multi-view stereo reconstruction algorithms. In: Proceedings of the IEEE Computer Society Conference on Computer Vision and Pattern Recognition, vol. 1, pp. 519–526 (2006)
7. Detert, M., Johnson, E.D., Weitbrecht, V.: Proof-of-concept for low-cost and non-contact synoptic airborne river flow measurements. Int. J. Remote Sens. **38**, 2780–2807 (2017)
8. Ioli, F., Pinto, L., Passoni, D., Nova, V., Detert, M.: Evaluation of airborne image velocimetry approaches using low-cost UAVs in riverine environments. In: International Archives of the Photogrammetry, Remote Sensing and Spatial Information Sciences - ISPRS Archives. pp. 597–604. International Society for Photogrammetry and Remote Sensing (2020)
9. Fugazza, D., et al.: Combination of UAV and terrestrial photogrammetry to assess rapid glacier evolution and map glacier hazards. Nat. Hazard. **18**, 1055–1071 (2018)
10. Ioli, F., et al.: Mid-term monitoring of glacier's variations with UAVs: The example of the belvedere glacier. Remote Sens. **14**, 1–19 (2022)
11. Geissler, J., Mayer, C., Jubanski, J., Münzer, U., Siegert, F.: Analyzing glacier retreat and mass balances using aerial and UAV photogrammetry in the Ötztal Alps, Austria (2021)
12. Attività glaciologiche - Fondazione Montagna sicura - Rutor Intro. http://app.fondazionemontagnasicura.org/multimedia/crgv/default.asp?principale=32&indice=32_33_91&sezione=90. Accessed 23 May 2022
13. Badino, F., et al.: 8800 years of high-altitude vegetation and climate history at the Rutor Glacier forefield, Italian Alps. Evidence of middle Holocene timberline rise and glacier contraction. Quat. Sci. Rev. **185**, 41–68 (2018)
14. Strigaro, D., Moretti, M., Mattavelli, M., Frigerio, I., de Amicis, M., Maggi, V.: A GRASS GIS module to obtain an estimation of glacier behavior under climate change: a pilot study on Italian glacier. Comput. Geosci. **94**, 68–76 (2016)
15. Villa, F., Tamburini, A., Sironi, S., Maggi, V.: Volume decrease of Rutor Glacier (Western Italian Alps) since little ice age: a quantitative approach combining GPR, GPS and cartography EPICA-European Project for Ice Coring in Antarctica View project POLLiCE View project (2008)
16. Software VERTO2k E VERTO3k—IGM E-Commerce Site. https://www.igmi.org/en/descrizione-prodotti/elementi-geodetici-1/software-verto-2k-3k. Accessed 23 May 2022
17. Avionic System Design Services - Digisky. https://www.digisky.it/. Accessed 20 May 2022
18. High Resolution Aerial Imagery & Photography Cameras - Phase One. https://geospatial.phaseone.com/cameras/ixm-rs150f/. Accessed 23 May 2022
19. Pleiades - eoPortal Directory - Satellite Missions. https://earth.esa.int/web/eoportal/satellite-missions/p/pleiades. Accessed 20 May 2022
20. Geoportale SCT - Dati territoriali Regione Valle d'Aosta. https://geoportale.regione.vda.it/. Accessed 20 May 2022